Available online at www.sciencedirect.com

ScienceDirect

Energy Procedia 142 (2017) 1282–1287

Energy Procedia

www.elsevier.com/locate/procedia

9th International Conference on Applied Energy, ICAE2017, 21-24 August 2017, Cardiff, UK

Dynamic Modelling and Control of a Reciprocating Engine

Hector Bastida[a*], Carlos E. Ugalde-Loo[a*], Muditha Abeysekera[a]

Cardiff School of Engineering, Cardiff University, Queens Building, The Parade, Cardiff CF243AA, UK

Abstract

Nowadays energy systems should be considered as integrated energy systems (IESs), where interactions between different energy vectors affect each other. A good performance of the whole system depends on the adequate behaviour of each individual element as undesired dynamics may propagate from one element to another. Due to the system complexity, a common practice is to employ steady-state models. Although such an approach is valuable as it provides significant insight into the system behaviour, it may hide inherent coupling characteristics as the dynamics are not considered. To ensure the satisfactory performance of each component, dynamic models are not only required, but essential. With a truly dynamic model it is possible to clearly understand how the system is affected by different operating conditions, load variations and disturbances over time, which in turn enables an effective control system design. Following this line, this paper presents a mathematical model, based on the mean value approach, of a reciprocating engine, which is used in combined heat and power units – key component of an IES. Although the system is non-linear, it is shown that a single-input single-output linear system can be derived and, thus, a frequency domain representation suitable for control system design can be obtained. The system has been developed in MATLAB/Simulink. Simulation results show that the designed linear controller is capable of ensuring a good performance of the reciprocating engine non-linear model.

Peer-review under responsibility of the scientific committee of the 9th International Conference on Applied Energy.

Keywords: Reciprocating engine; Non-linear dynamic model; Integrated energy system; Frequency domain; Control system design

1. Introduction

Combined heat and power (CHP) is a term applied to power generation systems which harness the excess heat generated by combustion processes. The reciprocating internal combustion engine is one of the most common prime movers used to produce mechanical power in CHP units. Given that the use of CHPs in integrated energy systems (IES) has increased to be able to cope effectively with energy demand growth and climate change, the understanding of the coupling behaviour of a CHP with other elements in the IES is essential.

* Corresponding author. Tel.: +44-0292-087-0675. *E-mail address:* Ugalde-LooC@cardiff.ac.uk

1876-6102
Peer-review under responsibility of the scientific committee of the 9th International Conference on Applied Energy.
10.1016/j.egypro.2017.12.486

IES elements such as CHP and heat exchanger units have been thoroughly investigated in a steady-state regime using the energy hub approach [1, 2]. The dynamic modelling of simple cylinder reciprocating engines has been carried out in [3]. However, speed control for CHP units is still an underdeveloped topic. The speed of a synchronous generator linked to a crankshaft engine is required to be constant so that frequency variations in the generated electrical energy are avoided. Due to the large variety of operating points, wide loading range, non-linearities in the combustion process and large parametric uncertainties, control system design becomes a challenging task. The bridge this gap, a dynamic model of a reciprocating engine is developed in this paper (shown in Fig. 1), which is an initial step towards obtaining a suitable model for a CHP. A non-linear engine model has been derived from first principles. Control system design is performed in the frequency domain following system linearisation. As it will be shown, a good performance of the non-linear model is achieved upon disturbances and irrespectively of the system loading.

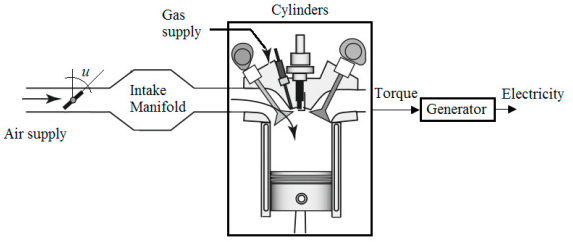

Fig. 1. Schematic of reciprocating engine [4].

Nomenclature

A	area of throttle valve (m^2)	ω	speed (s^{-1})	H	lower heating value (J)
q	mass flow rate (kg/s)	η_v	volumetric efficiency (%)	P_e	electric power (W)
k	air specific heat ratio (-)	J	inertia (kg m^2)	η_e	electric efficiency (%)
R	gas constant (J/kg K)	V	volume (m^3)	A/F	air/fuel ratio (-)
T	temperature (K)	N	revolutions per cycle (-)	T	torque (Nm)
p	pressure (Pa)	η_c	combustion efficiency (%)	b	damping (N s)

2. Non-linear reciprocating engine model

In this section, the mean value model (MVM) describing a gas engine is presented. Unlike classical models of reciprocating combustion engines, the MVM approach neglects the engine's discrete cycles and assumes that all effects involved in the process are carried out over the combustion/power generation cycle. In an MVM, time t is the independent variable in the differential equations representing the process – as opposed to the crankshaft angle ϕ in classical models [3]. In a gas engine, air is supplied at a certain pressure and mixed with gas at a constant ratio to produce combustion in the cylinders. Mechanical energy is then generated by the piston movements. The motion generated during combustion is transmitted to the crankshaft engine to produce rotational speed.

2.1. Throttle valve

The air flow of a compressible and ideal gas through an orifice is calculated with Bernoulli's equation [5, 6]:

$$q_i(t) = c_d[1-\cos(u)]\frac{\pi}{4}D^2\frac{p_{in}}{\sqrt{RT_{in}}}f(p_{in},p_{out}), \quad 0° \le u \le 90° \tag{1}$$

The air flow is adjusted by the opening of the throttle valve (u) from 0º to 90 º. This controls the air supply. A non-linear function establishes the relation between the input and output pressures according to [5]:

$$f(p_{in},p_{out}) = \begin{cases} \sqrt{k\left[\frac{2}{k+1}\right]^{\frac{k+1}{k-1}}} & p_{out} \le p_{cr} \\ \left[\frac{p_{out}}{p_{in}}\right]^{\frac{1}{k}}\sqrt{\frac{2k}{k-1}\left[1-\left(\frac{p_{out}}{p_{in}}\right)\frac{k-1}{k}\right]} & p_{out} > p_{cr} \end{cases} \tag{2}$$

In (2), when the value of p_{out} is less than $p_{cr} = (2/k + 1)^{k/k+1}p_{in}$, a choked (subsonic) mass flow occurs – otherwise a non-linear mass flow variation exists [5].

2.2. Intake manifold

The air supplied to the engine passes through a fixed volume (receiver). The intake manifold delivers a constant volume of air to the cylinders according to the engine's speed requirements. It is assumed that there is no heat or mass transfer through the receiver walls. The mass-balance equation is given by

$$\frac{d}{dt}m = q_{in} - q_{cyl} \tag{3}$$

Using (3) and considering that air is a compressible gas, the air pressure inside the intake manifold is described by:

$$\dot{p}_{out}(t) = \frac{RT_{in}}{V}\left[q_{in} - q_{cyl}\right] \tag{4}$$

2.3. Engine mass flow

The engine behaviour may be approximated as a volumetric pump [5, 7]. The air mass flow needed to produce combustion is defined by the following speed-density equation:

$$q_{cyl} = \frac{\eta_v p_{out} V_d \omega}{2\pi NRT} \tag{5}$$

The intake manifold pressure and the engine speed are the dynamic variables that govern the required air mass flow. Due to the limited dwell time of the air in the receiver the system is considered adiabatic: there is no temperature change in the air.

2.4. Generated power

Modern fuel injection systems maintain a constant relation between air and fuel mass flows (*A/F*) to achieve a volumetric efficiency without changes. Density and mass flow measurements of injected air are used to control fuel injection [8, 9]. For simplicity, *A/F* is kept constant. Thus, the power produced by the gas engine can be obtained with

$$P = \eta_c H q_f = \eta_c H q_{cyl}(F/A) = \frac{\eta_c \eta_v p_{out} V_d \omega H (F/A)}{2\pi NRT_{in}} \tag{6}$$

2.5. Rotational dynamics

The crankshaft engine is linked to a synchronous generator with inertia J and damping b. The mechanical energy generated by the engine acts as a prime mover for the generator to produce electricity. In the proposed model, only mechanical dynamics are considered, where the torque ($T_m = P_e/\omega$) produced by combustion is calculated using the electric efficiency of the generator:

$$\dot{\omega} = \frac{1}{J}[(T_m - T_e) - b\omega] = \frac{1}{J}\left[\left(\frac{\eta_v \eta_c \eta_e p_{out} V_d H(F/A)}{2\pi NRT_{in}} - T_e\right) - b\omega\right] \tag{7}$$

Thus, the differential equation describing pressure is defined by:

$$\dot{p}_{out}(t) = \frac{RT_{in}}{V}\left[c_d[1-\cos(u)]\frac{\pi}{4}D^2\frac{p_{in}}{\sqrt{RT_{in}}}f(p_{in}, p_{out}) - \frac{\eta_v p_{out} V_d \omega}{2\pi NRT}\right] \tag{8}$$

2.6. Case study

The case study shown in this paper considers a TCG 2020 V20 CHP unit, with parameters shown in Table 1 [10]. Since mechanical parameters are not available, the following values have been used: J =10 kg m^2 and b = 0.5 Ns. Volumetric efficiency η_v for combustion engines is usually within 0.8-0.9, while combustion efficiency η_c lies within 0.95-0.98 [7]. The following efficiency values are adopted: η_v = 0.85 and η_c = 0.95.

The system has been built in MATLAB/Simulink (see Fig. 2(a)). Simulation results (not shown due to space limitations) demonstrate that a sonic input flow is not reached through the whole load range (*i.e.* the input flow is subsonic). Thus, the first case in (2) is considered for control system design. Following an evaluation of parameters in (7) and (8), and after adopting a state-space notation ($x_1 = p_{out}$, $x_2 = \omega$), the reciprocating engine model is given by:

$$\dot{x}_1 = 1.4535\times10^8[1-\cos(u)] - 0.0595x_1x_2 \tag{9}$$

$$\dot{x}_2 = 0.0132x_1 - 2T_e - 0.05x_2 \tag{10}$$

Table 1. CHP parameters.

Variable	Value	Units	Variable	Value	Units
Valve diameter D	0.3	m^3	Input temperature T_{in}	290	K
Valve discharge coefficient c_d	0.8	-	Intake manifold volume V	0.1	m^3
Air specific heat ratio k	1.4	-	Natural Gas LHV H	5.4	MJ
Input pressure p_{in}	1301	kPa	Air-fuel ratio A/F	12	-
Displacement volume V_d	0.88	m^3	Electric efficiency η_e	0.43	-
Gas constant R	286.9	J/kg K	Generator damping b	0.5	N s

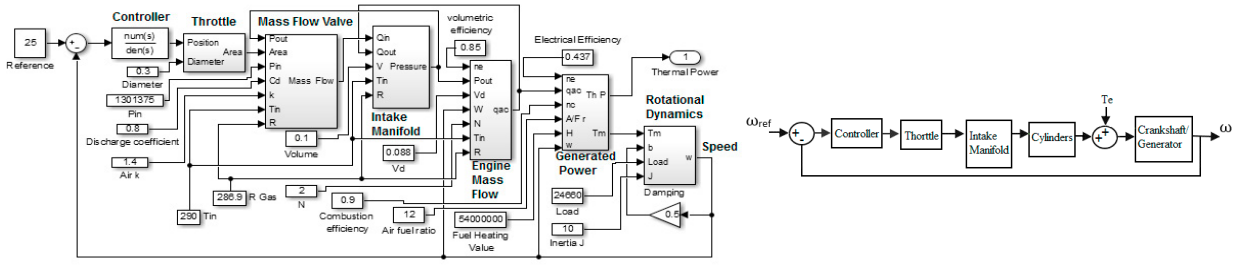

(a) (b)

Fig. 2. (a) Non-linear model implemented in MATLAB/Simulink. (b) Closed-Loop control scheme.

3. Controller design

The main target of a CHP is to produce enough energy to move the synchronous machine at a specific speed set-point and thus generate electricity at a certain frequency. A constant speed output of the crankshaft engine is therefore a critical issue for the adequate CHP performance. A suitably designed closed-loop controller is necessary to meet such requirement, while also rejecting dynamic load changes and disturbances (see Fig. 2(b)).

Since the system is non-linear, it is thus linearised at different operating points using a Taylor series expansion. The gradients of (9) and (10) are computed and evaluated in steady-state (x_s). The linearised plant is given by:

$$\begin{bmatrix}\Delta\dot{x}_1\\ \Delta\dot{x}_2\end{bmatrix}=\begin{bmatrix}\frac{\partial f_1}{\partial x_1} & \frac{\partial f_1}{\partial x_2}\\ \frac{\partial f_2}{\partial x_1} & \frac{\partial f_2}{\partial x_2}\end{bmatrix}_{x_s,u}\begin{bmatrix}\Delta x_1\\ \Delta x_2\end{bmatrix}+\begin{bmatrix}\frac{\partial f_1}{\partial u}\\ \frac{\partial f_2}{\partial u}\end{bmatrix}_{x_s,u}[\Delta u]=\begin{bmatrix}-0.0595x_{2,s} & -0.0595x_{1,s}\\ 0.0125 & -0.05\end{bmatrix}\begin{bmatrix}\Delta x_1\\ \Delta x_2\end{bmatrix}+\begin{bmatrix}1.4535\times10^8\\ 0\end{bmatrix}[\sin u_s],\quad \Delta y=\begin{bmatrix}0 & 1\end{bmatrix}\begin{bmatrix}\Delta x_1\\ \Delta x_2\end{bmatrix} \tag{11}$$

where f_1 and f_2 are given by (9) and (10), respectively. The state-space representation provided in (11), where the system output is $x_2 = \omega$, can be represented by a transfer function model as:

$$G(s)=\frac{1911500\sin(u_s)}{s^2+(0.05+0.0595x_{2,s})s+(0.003x_{2,s}+7.8282\times10^{-4}x_{1,s})} \tag{12}$$

The non-linear model previously built in MATLAB/Simulink is used to vary the loading conditions from no-load to full load in steps of 10% loading while keeping a constant speed of $\omega = 25$ s^{-1} ≈ 157 rad/s [10]. This enables the calculation of steady-state values for pressure ($x_{1,s}$) and for the opening position of the throttle valve (u_s). For the system under study, the maximum load is $T_e = 82200$ Nm [10]. Steady-state values are shown in Table 2.

Fig. 3(a) shows the frequency response (Bode plot) of $G(s)$ as a function of p_{out} and u, with $\omega = 25$ s^{-1}. The desired performance specifications are a settling time t_s = 10 s and a maximum overshoot of 10%. Since $G(s)$ represents a family of 2nd order systems, these specifications are easily translated into the frequency domain. To meet the desired performance, a phase margin of at least 60º and a bandwidth of 2.5 rad/s (according to $\omega_{bw} = 4/t_s$) are required [6].

Table 2. Case study. Steady-state (pressure, opening valve input) values at a constant speed of $\omega = 25$ s^{-1} ≈ 157 rad/s.

Load Torque [Nm]	Intake Manifold Pressure [Pa]	Opening Valve Input [°]	Load Torque [Nm]	Intake Manifold Pressure [Pa]	Opening Valve Input [°]
8220	64780	2.1	49320	393700	5.12
16440	129786	2.95	57540	450572	5.5
24660	193815	3.6	65760	526378	5.92
32880	260750	4.5	73980	576815	6.25
41100	321881	4.65	82200	649400	6.6

A suitable controller for each $G(s)$ was designed using Bode-shaping techniques. However, the controller that offers the best performance for all plants (designed for the smallest loading, $T_e = 8220$ Nm, as in Table 2) is given by:

$$C(s) = k_p \frac{1}{s} \cdot \frac{n_1(s)}{z_1(s)} = 2\times10^{-5} \frac{1}{s} \cdot \frac{s^2 + 1.538s + 48.48}{0.004s^2 + 0.1333s + 1} \tag{13}$$

Fig. 3(b) shows the open loop frequency response of the family of transfer functions $G(s)$ when controller (13) is applied. To design (13), the system poles in (12) (given $T_e = 8220$ Nm and thus $x_{1,s} = 64780$ Pa, $x_{2,s} = 25$ s^{-1}, $u_s = 2.1°$) were cancelled with zeros located at the same position. Then, a 2nd order system behaviour with a damping factor of 1 (*i.e.* no overshoot) and a phase margin ≈90º was achieved. To do this, a natural frequency of 15 rad/s was chosen for z_1 in (13). The last step was to modify the bandwidth to achieve the required t_s by adding a proportional gain k_p. It should be emphasised that an integral action was also included to the controller to eliminate the steady-state error.

Fig. 4(a) shows the frequency response of the open loop compensated systems $C(s)G(s)$. The closed-loop step responses are shown in Fig. 4(b). As it can be seen, a compromise must be made to meet the overshoot and settling time specifications. A slower time response (with t_s =15 s) should be adopted to avoid an overshoot greater than 10%.

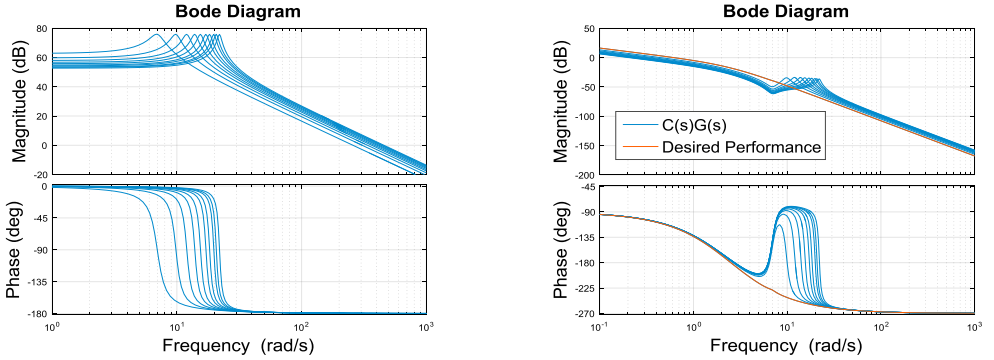

Fig. 3. (a) Bode plot of the open loop plant $G(s)$ (left). (b) Bode plot of $C(s)G(s)$ and desired performance (right).

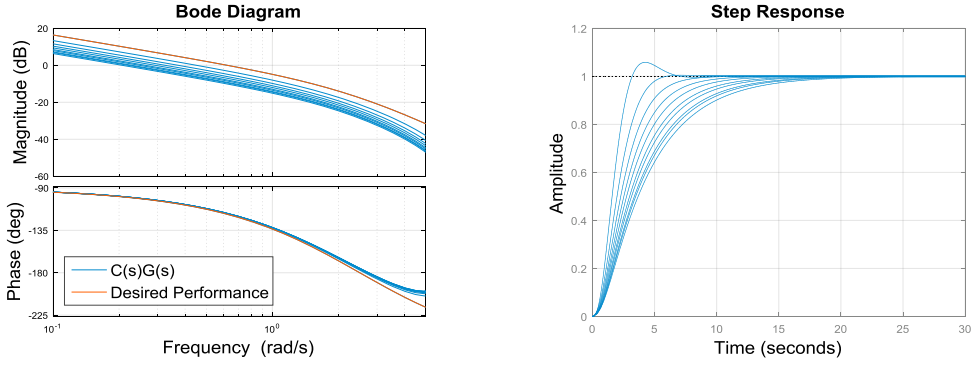

Fig. 4. (a) Bode plots for frequencies below 5 rad/s (left). (b) Closed-loop step response of $C(s)G(s)$ (right).

4. Simulation results

To verify the system performance when the designed controller (13) is employed, a closed-loop system simulation was performed in MATLAB/Simulink using the non-linear model (presented in Section 2). It should be highlighted that since the controller has no information of the system loading as a result of the linearisation exercise, the system exhibits a slow response. The controller was modified so that a faster response is achieved without compromising system stability. A proportional gain was added to the controller so that $C_1(s) = K_p C(s)$, with $K_p = 20$. Fig. 5(a) shows the closed-loop response of the system for $T_e = 8220$ Nm and when either $C(s)$ or $C_1(s)$ are used. As it can be seen, the performance achieved by $C_1(s)$ is significantly better compared to that afforded by $C(s)$. Fig 5(b) shows the closed-loop performance when the system operates at different loads (25, 50 and 100% of full load) and $C_1(s)$ is used. The system is perturbed, with changes in the operating load (10%) occurring at 750, 900, 1100 and 1300 s into the simulation and a 30% perturbation in load occurring during a period of 5 s starting at 530 s. As it can be observed, the performance of the system is maintained irrespectively of the system loading and upon disturbances.

It should be highlighted that the engine model presented in Section 2, for simplicity, considers the efficiencies as constant values. However, simulation results are considered valid as specific operating points have been examined.

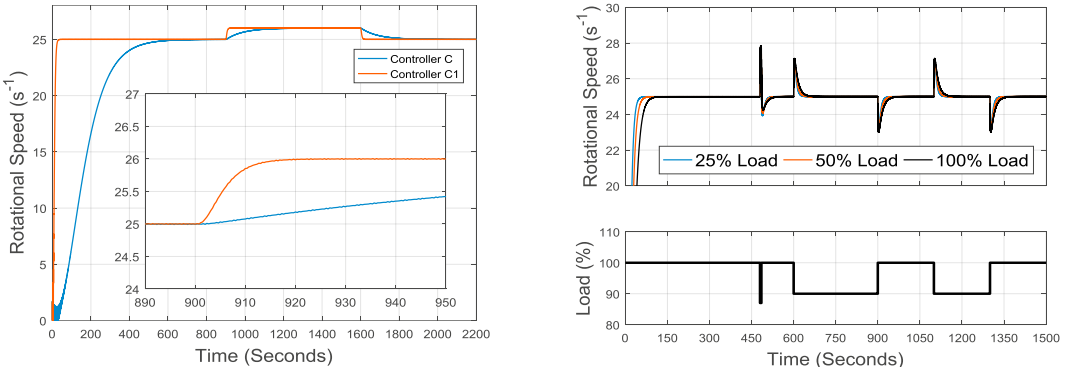

Fig. 5. (a) Comparison between controller $C(s)$ and $C_1(s)$ (left); (b) Engine performance under different loads (right).

5. Conclusions

In this paper, a dynamic non-linear model of a reciprocating engine was developed applying the MVM approach. Operating points at different loading conditions have been obtained by implementing the non-linear model in MATLAB/Simulink. Using system linearisation, a transfer function representation was derived, enabling linear control system design in the frequency domain. A good performance for different operating points was achieved in the non-linear simulation model with a simple linear controller, which, in addition, ensured disturbance rejection while the rotational speed reference was adequately followed. However, volumetric, combustion and electric efficiencies, currently kept as constant, should be considered to be variable to obtain more accurate results.

It should be emphasised that the work presented in this paper is an initial (but essential) step towards the dynamic modelling and control of an IES featuring CHP units. Although the presented engine model employs parameters of a real system, experimental data for this specific representation is not available in the open literature. As part of future work, the performance of the model presented in this paper will be validated against experimental datasets obtained from the facilities available in the University of Warwick.

Acknowledgements

The work presented in this paper was funded by the National Council for Science and Technology and the Energy Ministry of Mexico (CONACyT-SENER). This work was also supported by FLEXIS – a project part-funded by the European Regional Development Fund (ERDF) through the Welsh Government.

References

[1] Abeysekera, M., Wu, J., 2015. Method for Simultaneous Power Flow Analysis in Coupled Multi-vector Energy Networks. The 7th International Conference on Applied Energy (ICAE2015) 75, 1165–1171.
[2] Geidl, M., Andersson, G., 2005. A modeling and optimization approach for multiple energy carrier power flow. 2005 IEEE Russia Power Tech. pp. 1–7.
[3] Zadfiya, R.L., Barve, J., Unziya, V.H. Modelling, simulation and validation of reciprocating engine. Nirma University International Conference on Engineering (NUiCONE), 2015. pp. 1–5.
[4] Fan, J., Wu, Y., Ohata, A., Shen, T., 2016. Conservation law-based air mass flow calculation in engine intake systems. Sci. China Inf. Sci. 59, 112210.
[5] Guzzella L, Onder C. Introduction to Modelling and Control of Internal Combustion Engine Systems, 2nd ed. Berlin: Springer; 2009.
[6] Ogata, K. System Dynamics, 4th ed. Upper Saddle River, NJ: Pearson; 2003.
[7] Heywood, J. Internal Combustion Engine Fundamentals, 1st ed. New York: McGraw-Hill Education; 1988.
[8] Ebrahimi, B. *et al.* A parameter-varying filtered PID strategy for air–fuel ratio control of spark ignition engines. Control Engineering Practice 2012; 20. p. 805–815.
[9] Ebrahimi, B. *et al.* A Systematic Air-fuel Ratio Control Strategy for Lean-burn SI Engines. IFAC Proceedings Volumes, 3rd IFAC Workshop on Engine and Powertrain Control, Simulation and Modeling 2012;45. p. 296–301.
[10] MWM gas engine TCG 2020. Available at: https://issuu.com/mwm_energy/docs/mwm_lb_tcg_2020_en/1.